Plant Mol Biol (2007) 63:731–744
DOI 10.1007/s11103-006-9105-z

Mutations in the *TORNADO2* gene affect cellular decisions in the peripheral zone of the shoot apical meristem of *Arabidopsis thaliana*

Wei-Hsin Chiu · John Chandler · Gerda Cnops · Mieke Van Lijsebettens · Wolfgang Werr

Received: 25 August 2006 / Accepted: 26 October 2006 / Published online: 16 February 2007

Summary An EMS (ethyl methanesulfonate) mutagenesis effector screen performed with the *STM:GUS* marker line in *Arabidopsis thaliana* identified a loss-of-function allele of the *TORNADO2* gene. The histological and genetic analyses described here implicate *TRN2* in SAM function, where the peripheral zone in *trn2* mutants is enlarged relative to the central stem cell zone. The *trn2* mutant allele partially rescues the phenotype of *shoot meristemless* mutants but behaves additively to *wuschel* and *clavata3* alleles during the vegetative phase and in the outer floral whorls. The development of carpels in *trn2 wus-1* double mutant flowers indicates that pluripotent cells persist in floral meristems in the absence of *TRN2* function and can be recruited for carpel anlagen. The data implicate a membrane-bound plant tetraspanin protein in cellular decisions in the peripheral zone of the SAM.

Keywords Shoot apical meristem · Peripheral zone · *STM* gene · *Arabidopsis*

Introduction

Development and growth of the aerial plant body depends on activity of the shoot apical meristem (SAM). Established early during embryogenesis, the SAM maintains a source of pluripotent stem cells throughout the plant life cycle (Sussex 1989). A delicate balance exists between the maintenance of stem cells in the central zone and the release of cells at the periphery for reiterated organ formation throughout the life cycle of the plant. In *Arabidopsis*, the *WUSCHEL* (*WUS*) homeobox gene acts cell-autonomously in a so-called stem cell organizing centre (OC) (Mayer et al. 1998) to maintain stem cell homeostasis, its expression being restricted to a few cells of the L3 layer in the centre of the SAM. *WUS* is antagonized by CLAVATA (CLV) signalling (Schoof et al. 2000; Waites and Simon 2000). Acting in a single pathway, the three *CLV* genes (*CLV1-3*) encode a heterodimeric trans-membrane receptor kinase consisting of CLV1/2 (Clark et al. 1997) and its corresponding 95 aa polypeptide ligand CLV3 (Fletcher et al. 1999), which is expressed at the apical tip of the SAM. The *CLV3* expression domain located above the *WUS*-positive OC is considered to depict the stem cell domain in the SAM of the model species *Arabidopsis thaliana*.

The *SHOOT MERISTEMLESS* gene contributes an essential function for establishment and maintenance of the *Arabidopsis* SAM (Endrizzi et al. 1996). Plants homozygous for *stm* loss of function alleles fail to establish a functional SAM during embryogenesis (Long et al. 1996). *STM*, similar to *WUS*, encodes a homeodomain transcription factor albeit from a different subfamily. *STM* gene activity is exclusive for the SAM from the embryonic to the reproductive phases (Long et al. 1996). In contrast to *WUS* (Mayer et al. 1998) and *CLV3* (Fletcher et al. 1999) expression patterns, *STM* is not confined to sub-domains of the SAM but is expressed throughout the meristem and

W.-H. Chiu · J. Chandler · W. Werr (✉)
Institute of Developmental Biology, University Cologne, Gyrhofstr. 17, Cologne D-50923, Germany
e-mail: werr@uni-koeln.de

G. Cnops · M. Van Lijsebettens
Department of Plant Systems Biology, Flanders Interuniversity Institute for Biotechnology, Ghent University, Technologiepark 927, Ghent B-9052, Belgium

down-regulated when cells acquire primordial fate at the SAM periphery (Long et al. 1996). The loss of *STM* transcription in the P_0 leaf is one of the earliest molecular features that distinguishes meristematic cells from those recruited for lateral organs. *STM* transcription therefore can be considered as a marker for meristematic cell fate, which is mimicked by fusions of the *STM* promoter with the glucuronidase marker gene (*STM:GUS*) (Kirch et al. 2003).

An open question concerning SAM function is how cells acquire primordial fate at the meristem periphery and lose their meristematic identity before differentiating into lateral organs. This question relates to the diversity of plant architecture, phyllotaxy and the perception of positional information at the peripheral zone of the SAM. Recent data provide evidence that auxin is transported towards founder cells of new organ primordia involving changes in the distribution of PIN proteins at the plasma membrane (Reinhardt et al. 2003). Auxin transport, therefore, provides evidence for alterations in cell polarity in the course of the acquisition of primordial fate, although the molecular basis for this remains to be established. An emerging scheme for signalling in animal cells incorporates specialized membrane microdomains, which often contain master organizers in so-called tetraspanin-enriched microdomains (TEMs) (Hemler 2005; Levy and Shoham 2005). The *Arabidopsis tornado2/ekeko* alleles represent mutations in a tetraspanin-like protein and cause severe distortions throughout plant development, such as severely twisted leaves (Cnops et al. 2000; Olmos et al. 2003). The plant TRN2 protein shares essential characteristics with its animal tetraspanin counterparts, such as a small N- and a larger C-terminal extra-cellular loop, whereas the intracellular domains at the N- or C-terminus are small (Olmos et al. 2003; Cnops et al. 2006). One difference between plant and animal tetraspanins may be the organization of the second large extra-cellular loop where the α-helical organisation is well-conserved although a conserved cysteine scaffold in animal tetraspanins (Hemler 2005) has evolved some differences in plants. Potentially, tetraspanin-like proteins in plants could therefore provide similar functions to those in animals where they contribute to signal transduction, cell polarity or cell-to-cell communication. The recent finding that *TRN1* encodes a Leucine-rich repeat (LRR) protein of the ribonuclease inhibitor subfamily (Carland and McHale 1996, Cnops et al. 2006), which acts in the same pathway with *TRN2* further substantiates a function for plant tetraspanin-like proteins in signal transduction (Cnops et al. 2006).

Here, we describe the analysis of a mutant obtained from a transcriptional effector screen performed with a *STM:GUS* marker line following EMS mutagenesis. The mutant is characterised by an altered *STM:GUS* expression domain and SAM morphology. The responsible mutation was shown to be allelic to *trn2* and provides evidence that plant tetraspanin-like proteins such as TRN2 contribute to SAM function. Molecular markers indicate that the size of the central stem cell zone is unaffected although the SAM is significantly enlarged compared to that of the wild type.

Materials and methods

EMS mutagenesis, screening and genetics

The construction of the *STM:GUS* marker line has been previously described (Kirch et al. 2003). For EMS mutagenesis (0.25%), 0.3 g homozygous *STM:GUS* transgenic seeds were soaked in 0.1% Tween 20 for 15 min and treated with 37 µl EMS in a total volume of 15 ml H_2O overnight. From a total of 5100 M_1 progeny, 4200 M_2 lines were established and subjected to analysis of the *STM:GUS* expression pattern. *Arabidopsis thaliana* seeds were sown on soil and kept at 4°C in the dark for 3 days before transfer to the greenhouse, where plants were grown under long-day conditions (16 h light) at 22°C. GUS staining was performed in 50 mM sodium phosphate buffer (pH 7.2), 2 mM potassium hexacyanoferrate, 0.2% Triton and 2 mM X-Gluc (5-bromo-4-chloro-3-indolyl-bD-glucuronic acid) overnight at 37°C and tissue was cleared in ethanol. For staining of nuclei, seedlings were stained in1 mg DAPI, 1% Tween for 4–8 h after vacuum infiltration (10′). Ultra-thin sectioning was performed as outlined for in situ hybridisations. The cell number was estimated by counting DAPI-stained nuclei of serial sections through wild type and *trn2-2*$_{3010}$ mutant apices. The mean cell number was estimated from 10 samples for each genotype. The cell number in wild type ranged between 157–273 nuclei detectable in 4–5 consecutive sections with a mean of 217, whereas the number of nuclei in 5–6 sections through *trn2-2*$_{3010}$ mutant apices was between 267 and 476 (mean 335).

Heterozygous M_2 progeny of lines 3010 and 145 were back-crossed to Columbia wild type to clean the genome from secondary EMS mutations. The *trn2-2*$_{3010}$ allele was propagated heterozygously, with progeny of crosses being mostly genotyped by DNA

sequencing of PCR products obtained with primers flanking the G to A mutation. Crosses of *trn2*$_{3010}$ with the *trn2-1* allele revealed a leaf phenotype in the F_1 generation, and *STM:GUS* staining (50% of the mutant progeny) showed a protruding SAM. All double mutants with *stm-1*, *stm-5*, *wus-1* and *clv3-2* were confirmed by PCR-based genotyping with the following primer pairs: *trn2-2*$_{3010}$ (CACTTAATCAGTCACGCCGAACTAC and GACGATAACAATCCGATAAGC), *stm-1* (GTCAATTCAAATCCCTCTC TC TA and GCTTTCCTTTCTTCCTCTTCTTC), *stm-5* (GAAGAAGAGGAAGAAAGGAAAGC and GC AATGCCAACATGAGCTAAC), *wus-1*(GCAAG CTCAGGTACTGAATGTG and CCTCCACCTAC GTTGTTGTAATTC) and *clv3-2* (TCCGGTCCAGT TCAACAACT and CTCCCGAAATGGTAAAAC).

Mapping

CAPS markers were used according to the protocol of (Konieczny and Ausubel 1993) to map the mutation in line 3010. Heterozygous *trn2*$_{3010}$ mutant plants (Columbia) were crossed to Landsberg *erecta* and 30 phenotypic progeny were selected in the F_2 generation. After genomic DNA extraction by the method of Kasajima et al. (2004), the mutation was associated to chromosome 5 by co-segregation of CAPS markers with the mutant phenotype and was fine-mapped with the markers LMYC6, MDA7, EG7F2, ATTED2. The corresponding linkage frequencies are indicated in Fig. 3A together with the relative position of each marker. Molecular information on these markers is available at TAIR DB (http://www.arabidopsis.org)

PCR amplification and DNA sequencing of the *trn2*$_{3010}$ allele

DNA extraction was performed according to the method of Kasajima et al. (2004). Two sets of overlapping primers (8f: TCTCTCTCTCAATTATTACCATT and 8r: GTAGAAAGATATCCGCTTTTA; 9bf: CGCCGAACTACTTTTTTG and 9br: GTGGCCTATATGGCTCAA) for the At5g 46700 coding sequence and the untranslated upstream and downstream regions were designed. About 25 ng of genomic *trn2*$_{3010}$ DNA was used as a PCR template using 0.2 µl Promega Taq polymerase (Promega Corporation, Madison, USA). The conditions used for PCR amplification were: 2 min at 94°C; 30 cycles of 15 s at 94°C, 30 s at 50°C for primers 8f and 8r and 51°C for 9bf and 9br, 2 min at 72°C, followed by 5 min at 72°C. Three independent *trn2-2*$_{3010}$ PCR products were sequenced for each primer set. The three *trn2* and the Columbia At5g46700 (http://www.tigr.org) sequences were aligned using the multiple sequence alignment programme ClustalW (http://www.searchlauncher.bcm.tmc.edu/multi-align/multi-align.html). DNA sequencing analysis was performed using the dideoxy chain termination method (Sanger et al. 1977). Prior to sequencing, PCR products were treated with the ExoSAP-IT kit from USB (Biolynx, Ontario, Canada). Thereafter, the treated PCR products were sequenced using fluorescent dye terminators from the cycle sequencing kit (Applied Biosystems, Foster City, USA) on an ABI3700 automatic DNA sequencer (Applied Biosystems, Foster City, USA). The raw output sequence data were analyzed using the Phred/Phrap software Ewing et al. 1998).

Sectioning and *in situ* hybridisation

Samples after DAPI staining and for non-radioactive in situ hybridization were dissected and fixed at 4°C overnight in 4% formaldehyde in phosphate-buffered saline, dehydrated in an ethanol series and embedded in paraffin wax (Paraplast plus, SIGMA). Paraffin wax-embedded tissue was sectioned with a Leica RM 2145 rotary microtome and mounted on coated slides (SuperFrost®Plus). Probes for in situ hybridization were cloned either in sense or antisense orientation relative to the T7 promoter or by direct addition of the T7 promoter to the reverse primer and then used as a template for synthesis of digoxigenin-labelled RNA probes by T7 RNA polymerase as described (Bradley et al. 1993) RNA in situ hybridization was performed according to the method of Jackson (1991). In situ probes for *STM*, *WUS*, *CLV3* and *LFY* were derived from the respective protein coding regions.

Light microscopy and image processing

Nomarsky images were taken using an *Axioskop* microscope in combination with an *Axiocam* camera (*Zeiss*, Germany). Pictures were digitised using *Axio Vision* software version 3.06 and processed using Adobe® Photoshop® version 7.0.

Real-time PCR

STM, *WUS* and *CLV3* transcript levels in wild type and *trn2*$_{3010}$ mutants were quantified by TaqMan® gene Expression Assays (Applied Biosystems). Synthesis of first strand cDNA was performed on total RNA (Chomczynski and Sacchi 1987) by SuperScriptII^{TM}

reverse transcriptase (Invitrogen) and diluted 8 times for quantification of *STM* transcript levels and 4 times to quantify *WUS* and *CLV3* expression. Expression of the *ACTIN2* (At3G 18780) gene was used as an endogenous control with appropriate primers obtained from Applied Biosystems. Real-time PCR reactions were performed using the ABI Prism HT7900 PCR machine and analysed with SDS software (version 2.2.1). Relative gene expression changes were compared according to Livak and Schmittgen (2001), DCt comparisons and *t*-tests were performed in Excel (Microsoft). All real-time PCR reactions were repeated 4 times with 3 independent *cDNA* syntheses originating from different RNA preparations and plant samples. Primer and FAM (6-carboxy-fluorescein) probes were *STM*: GCCGCTTATGTCAATTGTCAGAA and GACGAGCATGCCTCCTCTAG FAM-CCACCGGAGGTTGTG; *CLV3*: CAGATCTCACTCAAGCTCATGCT and CCAACC-CATTCACTTTCCATTTTCA, FAM-ACGTTCAAGGACTTTCC and *WUS*: GGATCATC-ATTACTCATCT GCACCTT and GCCACCACATTCTTCTTCTT CTTGA, FAM-TTCGATAG-AGCAAAGCCT. All FAM primers contained the non-fluorescent quencher (NFQ) at the 3′ terminus.

Results

Screen for *STM* effector mutants

To search for *STM* effector genes, we EMS-mutagenized a previously established homozygous *STM:GUS* line (Kirch et al. 2003) where glucuronidase enzyme activity reflected transcriptional activity of the *STM* promoter in the shoot meristem (Fig. 1A and C). After selfing of M_1 progeny, the M_2 generation was screened for differences in GUS expression at the early seedling stage. Among 4200 independent M_2 lines, a reduction or absence of *STM:GUS* activity was observed in

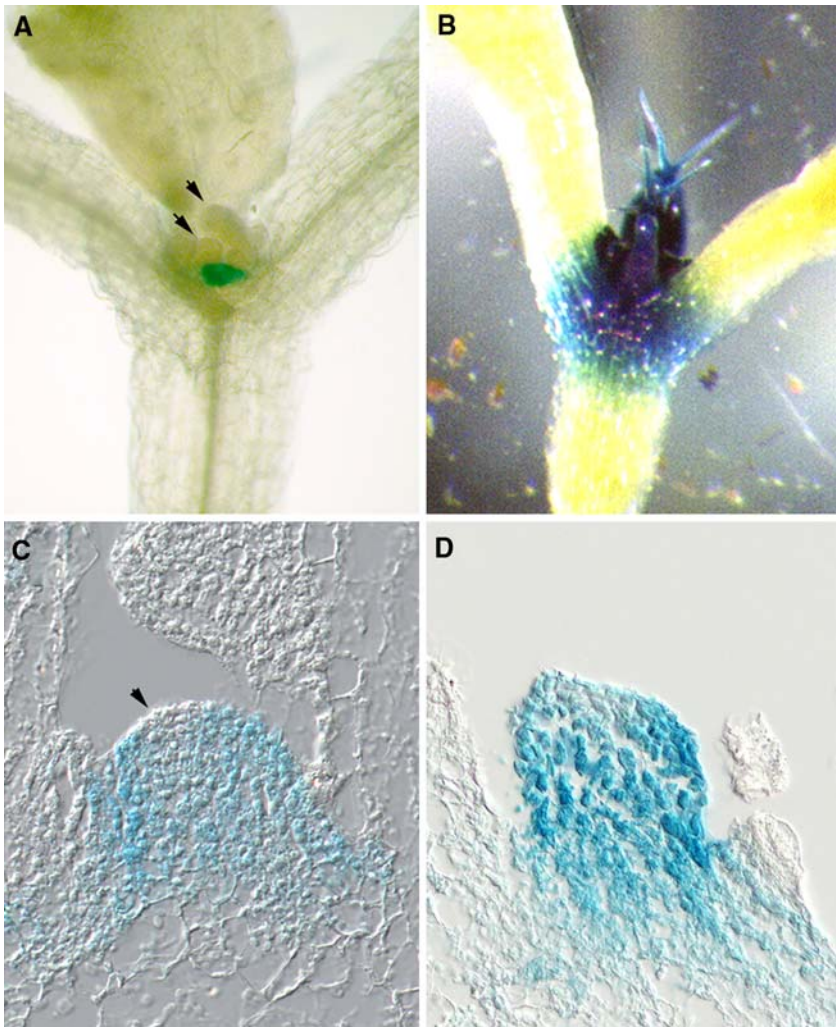

Fig. 1 STM:GUS expression pattern in wild type and line 3010 seedlings. (**A**) Whole mount of a *STM-GUS* transgenic seedling 11 days after germination with the frontal leaf primordium removed. The arrows mark the 2 youngest leaf primordia above the GUS-positive SAM. (**B**) Whole mount of a line 3010 M_2 seedling with a first normal trichome-bearing first leaf behind and an abnormal leaflet in front of the SAM. (**C**) Median section through a GUS-stained wild type SAM of *STM-GUS* transgenic line. The arrow indicates down-regulation in the incipient P_0 primordium (**D**) Median section through a typical protruding SAM in line 3010 flanked by non-stained leaf primordia. The twisted leaf to the right is leaving the plane of section. Plants depicted in (**A**/**B**) were stained overnight, whereas seedlings sectioned in (**C**/**D**) were stained briefly (6 h) to ensure meristem specificity. Scale bars = 50 mm

individual progeny of about 1% of lines and some of these loss-of-function lines are still under investigation. However, two lines showed an increase in GUS activity suggesting expansion of the *STM:GUS* expression domain. Subsequent genetic analyses including several back-crosses to purify the genome from secondary EMS mutations showed that the mutant phenotype in line 3010 (see Fig. 1B and D) segregated with a 3:1 ratio indicative of a single recessive mutant allele. In contrast, the mutant phenotype in a second line (145) did not show a segregation pattern compatible with a single locus trait or a double mutant combination. Further analysis therefore, focussed on line 3010, which is subject of analysis here. Compared in Fig. 1 are whole mounts and sections through wild type and mutant meristems comparing the *STM:GUS* expression pattern in wild type (Fig. 1A and C) with the mutant SAM (Fig. 1B and D) in seedlings 11 days after germination. A typical feature of line 3010 mutant seedlings was an enlarged apical dome, altered in shape and often protruding as depicted in Fig. 1D. To estimate cell number in wild type and mutant meristems we stained vegetative meristems with DAPI and counted nuclei in series of consecutive ultra-thin sections (7 mm) through 10 wild type and 10 mutant meristems 11 days after germination. The mean cell number in the wild type SAM was 217 cells compares with 335 in mutant line 3010 seedling meristems. The mutant meristem therefore contains over 40% more cells ($P = 0.003$). The median longitudinal sections depicted in Fig. 1C and D compare the *STM:GUS* domain in the wild type and abnormally shaped line 3010 apex. Based on the activity of the *STM* promoter all cells in the protruding mutant SAM have continued meristematic identity. However, interpretation of the GUS staining patterns in ultra-thin sections argues against ectopic *STM* promoter activity in primordia, although extended staining reactions (16 h) in the presence of potassium hexacyanoferrate sometimes also showed very weak background GUS activity outside the SAM. We can consequently not exclude that detection of the blue indigo precipitate differs slightly between whole mounts and ultra-thin sections. However, the increased GUS activity detected in line 3010 seedlings clearly relates to changes in the cell number in the SAM and possibly altered promoter activity.

Mutant phenotype

Homozygous 3010 mutant plants were subjected to a phenotypic analysis throughout their life cycle. Phenotypic differences from wild type development first became evident with the emergence of the first true leaves. All leaves were severely twisted and irregularly shaped (compare Fig. 2A and B) and many lacked large parts of the leaf lamina (see Fig. 2C). This twisting phenotype was not restricted to the vegetative phase but involved cauline leaves, the inflorescence stem and all floral whorls (Fig. 2E–H). In addition, the architecture of mutant flowers was distorted and was accompanied by reduced numbers of floral organs in the outer 3 whorls. This effect was least pronounced in the whorl of sepals (3.2 as against 4 in wild type) but the number of petals was reduced to 2.4 (4 in wild type) and on average, mutant flowers had only 3.5 stamens compared to 6 in wild type (summarized in Table 1). In contrast, all mutant flowers contained 2 carpels such as in wild type but in 52% of mutant flowers, both carpels remained unfused and ovules were exposed (see Fig. 2G). No siliques resulted from such unfused carpels later during development. In contrast, the remaining flowers with fused carpels developed siliques which were twisted and failed to fully elongate (Fig. 2H). However, these siliques produced no fertile seeds and reciprocal crosses with wild type plants revealed non-functionality of both male and female reproductive organs. Many aspects of the mutant phenotype in line 3010 were reminiscent of mutations at the *TRN1* and *TRN2* loci (Carland and McHale 1996; Cnops et al. 2000) or *ekeko* (Olmos et al. 2003), however, a shoot meristem phenotype as indicated by the *STM:GUS* reporter gene expression has not been previously described.

Mapping of the mutation in line 3010 and *trn2* allelism

The *STM:GUS* marker line used for EMS mutagenesis was established in the Columbia ecotype. To determine the chromosomal position of the *STM* effector mutation in line 3010, we crossed progeny of 3010 line with L. *erecta* and screened for recovery of the SAM phenotype based on *STM:GUS* expression in the F_2 generation. As in Columbia back-crossed plants the SAM and leaf phenotype in the hybrid Col/L*er* F_2 generation strictly co-segregated in a 3:1 ratio. Chromosome-specific CAPS markers firstly associated the mutation with chromosome 5 (Konieczny and Ausubel 1993). Fine mapping with additional markers further positioned the mutation on the long arm of chromosome 5 between markers LMYC6 and MDA7 as depicted in Fig. 3A. This chromosomal region spans approximately 6 Mb and contains the two linked loci *TRN1* and *TRN2*, both causing a similar phenotype to that of the mutation in line 3010.

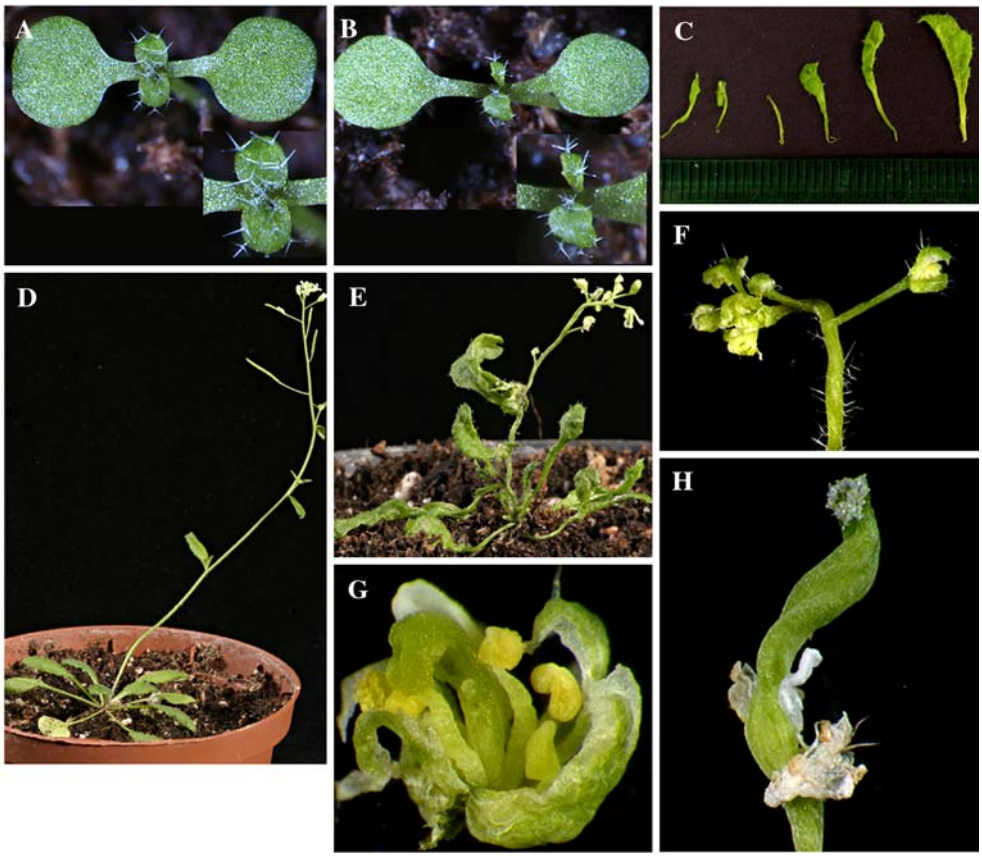

Fig. 2 Mutant phenotype of progeny of line 3010 after the first back-cross 2 leaf-stage wild type seedling. (**B**) Mutant seedling at the same developmental stage as in (**A**). Note the malformed leaves relative to the cotyledons in the close-up bottom right. (**C**) Consecutive leaves from a mutant plantlet. Note the absence of part or half of the leaf lamina (rightmost leaf) and the radialised leaf (third from the left). (**D**) Wild type plant with normal inflorescence. (**E**) Mutant progeny with a twisted inflorescence and a cauline leaf. (**F**) Tip of a 3010 inflorescence with multiple immature flowers. (**G**) Close-up of a mutant flower with unfused carpels. (**H**) Twisted style with normal looking stigma at the apical tip

To test for allelism, we pursued 2 strategies; firstly, genetic crosses were performed between the mutant 3010 line and *trn1-1* or *trn2-1* mutant alleles (Carland and McHale 1996, Cnops et al. 2000). Secondly, the *TRN1* and *TRN2* coding sequences were amplified by PCR from genomic DNA of homozygous mutant line 3010 seedlings and subjected to DNA sequence analysis. Both methods identified the mutation in line 3010 to be allelic to *trn2*. In crosses between heterozygous *trn2-1* and line 3010 plants, the mutant phenotype was recovered in the F_1 generation in a quarter of F_1 progeny as expected for the transmission of a single recessive locus. The same result was obtained in a second cross between line 3010 and the *trn2-2* allele. Transmission of the *STM-GUS* marker and GUS staining of F_1 trans-heterozygous *trn2-1/3010* or *trn2-2/3010* seedlings uncovered a similar increase in meristem size or SAM morphology as depicted for homozygous line 3010 seedlings SAM in Fig. 1D. The 3:1 seggregation in the F_1 generation and the reproducible change in SAM morphology obtained with two independent *trn2* alleles in combination with line 3010 argue against that secondary EMS mutations in the 3010 background contribute to the mutant phenotype. More importantly, however, the phenotype of the SAM in trans-heterozygous combinations of 3010 with 2 different *trn2* alleles, *trn2-1* and *trn2-2* substantiate a role of *TRN2* in SAM function.

The *TRN2* locus encodes a tetraspanin-like protein and EMS mutagenesis caused a G to A nucleotide substitution in the *TRN2* gene of line 3010 in the second coding exon resulting in a single glycine to

Table 1 Floral organ numbers

	Sepals	Petals	Stamens	Carpels	Carpels unfused
WT (n = 31)	4.0 ± 0	4.0 ± 0	6.0 ± 0	2.0 ± 0	0.0%
$trn2_{3010}$ (n = 39)	3.2 ± 0.8	2.4 ± 0.8	3.5 ± 1.0	2.0 ± 0	52.0%
clv3-2 (n = 34)	4.3 ± 0.4	4.1 ± 0.5	7.0 ± 0.9	[a]Many	0.0%
clv3-2 $trn2_{3010}$ (n = 33)	2.1 ± 1	1.9 ± 1.1	2.8 ± 2.8	[a]Many	27.0%
wus1 (n = 31)	3.7 ± 0.5	3.4 ± 1.0	1.6 ± 0.8	0.0	[b]ND
wus1 $trn2_{3010}$ (n = 27)	3.2 ± 0.8	2.4 ± 1.1	4.2 ± 1.1	2.0 ± 0	33.0%

[a] More than 4 carpels fused to a single style

[b] ND, not detectable

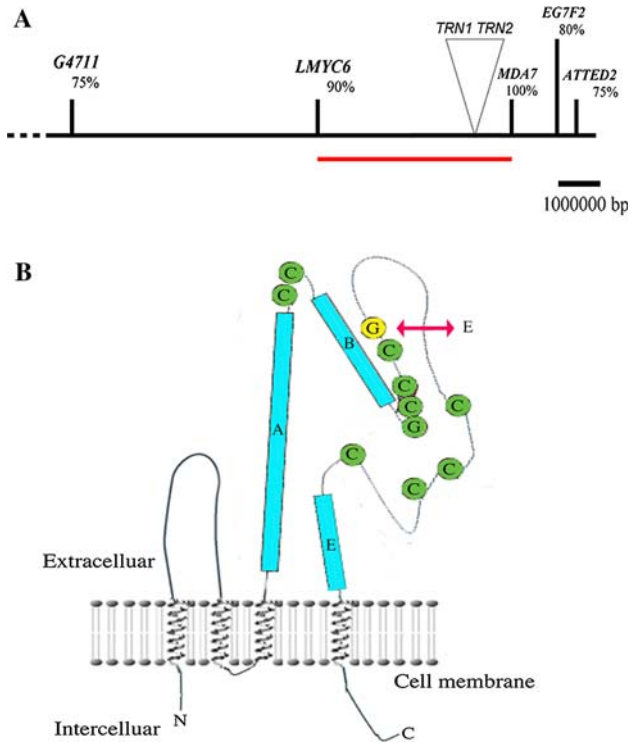

Fig. 3 Map position of the mutation in line 3010 and amino acid exchange in the TRN2 protein. (**A**) The 3010 mutation maps between the CAPS markers LMYC6 and MDA7 withn the red interval, which spans the *TRN1* and *TRN2* loci. (**B**) Structure of the TRN2 tetraspanin protein and position of the G to E amino acid exchange in the large extra-cellular loop based on the G to A nucleotide substitution in the *TRN2* gene. The boxes indicate conserved a-helices. Relative to the C-scaffold, the G to E exchange is close to a highly conserved GCC motif C-terminal to the central helix B

glutamic acid (G > E) amino acid exchange at position 81 of the TRN2 protein (Fig. 3B). The point mutation found in line 3010 genomic DNA is identical to that in the *trn2-2* allele (Cnops et al. 2006). The amino acid exchange is located in the second larger extra-cellular loop typical for tetraspanin proteins and flanks a Cys (C_{80}) residue conserved in all *Arabidopsis* relatives. This second extra-cellular loop contains a C-scaffold characteristic for tetraspanin proteins, although the absolute number of C residues and their relative position varies between animal and plant relatives. However, the replacement of the uncharged G residue flanking C_{80} with the negatively charged glutamic acid obviously is not tolerated at the functional level in *trn2-2* and the re-isolated *trn2-2*$_{3010}$ allele originating from our *STM-GUS* modifier screen.

Spatial transcription pattern of *TRN2*

To substantiate an interaction between *STM* and *TRN2* comparative RNA in situ hybridizations were performed to confirm a spatial overlap between the individual expression domains in the SAM (Fig. 4). *TRN2* transcriptional activity was detected in all types of meristems, whether vegetative, inflorescence and floral, where *STM* is co-expressed (compare Fig. 4A, B, C, to E or F). On the spatial level, the loss of *TRN2* function could therefore potentially affect *STM* activity. However, in contrast to *STM* transcriptional activity the expression of the *TRN2* gene is not exclusive to the SAM. Consistent with the twisted organ phenotype, transcripts are also detectable in lateral organ primordia as described recently by Cnops et al. 2006). *TRN2* transcripts in leaf primorida are preferentially found in vascular strands and at the distal tip of the leaflet. A section through a stage 3 flower (Fig. 4C) shows a continuous *TRN2* expression domain through the floral meristem into the flanking sepal primordia. Expression is also detected later during floral development as seen in stamens and carpels of stage 7 flowers (Fig. 4D). Although *TRN2* expression is not restricted to meristems, it overlaps with *STM* activity in the SAM.

Characterisation of the 3010 mutant SAM using molecular markers

To gain a deeper insight in the architecture of the *trn2-2*$_{3010}$ SAM, we applied different meristem-specific molecular markers in RNA in situ hybridisations. Firstly, the transcriptional activity of the endogenous *STM* gene was compared to the activity of the *STM:GUS* transgene marker and confirmed transcriptional activity of the endogenous *STM* gene throughout the enlarged apex (compare Fig. 4E to F). The expression domain is reminiscent of the *STM:GUS* expression pattern depicted in Fig. 1C and rules out differences due to the chimeric transgene marker. The *STM* expression pattern in wild type and *trn2*$_{3010}$ inflorescences is shown in Fig. 4G and H, respectively. The expression patterns are hard to compare, as *trn2*$_{3010}$ inflorescence shoots are severely twisted and the initiation of floral meristems does not follow a regular pattern. However, neither IM nor FM morphology nor quantification of the *STM* RNA suggests there are significant quantitative changes in *STM* expression between mutant and wild type inflorescences.

The organisation of the mutant SAM was addressed by the use of *WUS* and *CLV3* probes on sections of *trn2-2*$_{3010}$ mutant and wild type seedling meristems. Both probes were used to investigate whether possible differences exist in the central stem cell zone relative to the peripheral zone in the mutant SAM. Whereas

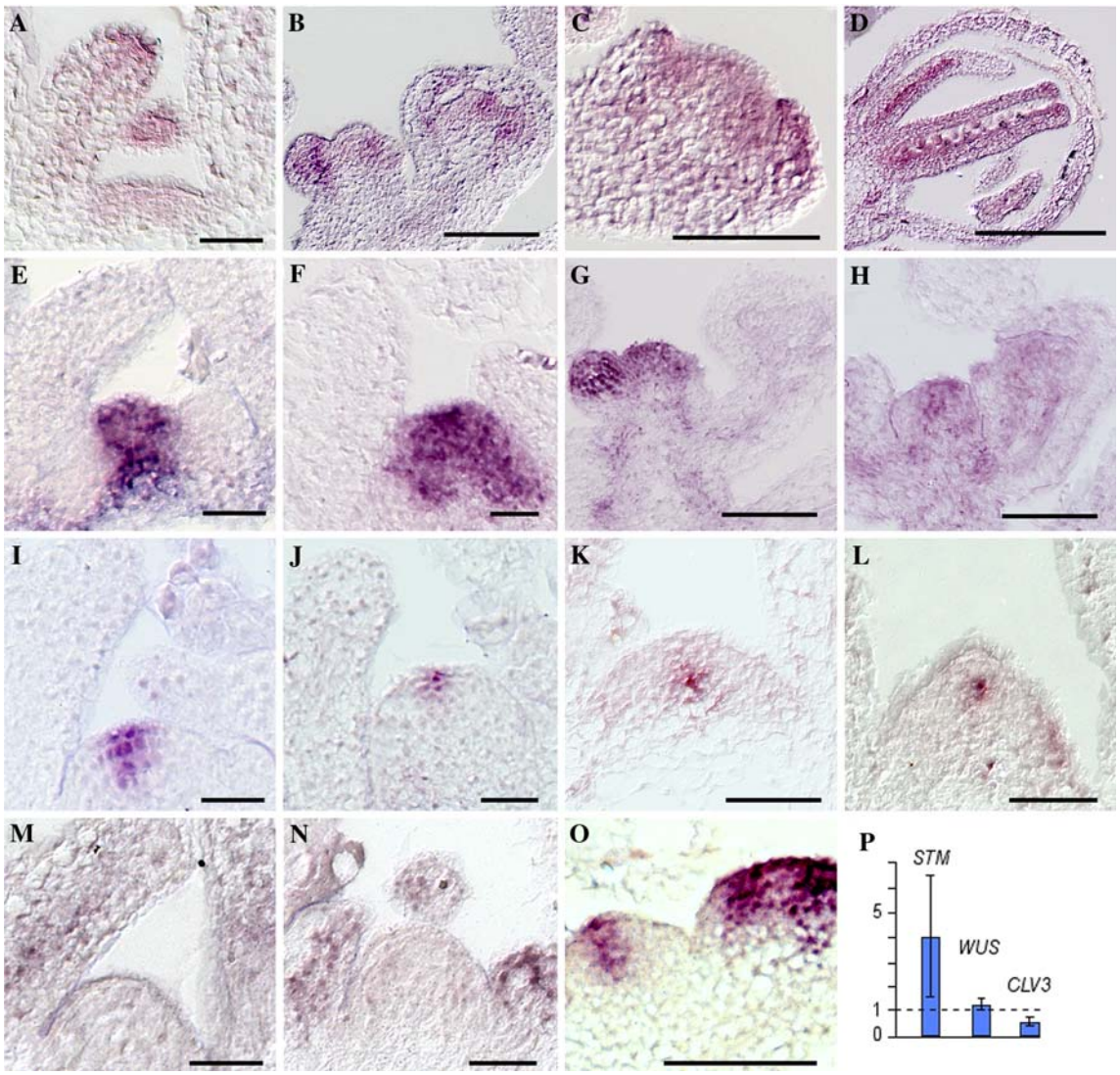

Fig. 4 RNA in situ hybridizations in wild type and *trn2*$_{3010}$ plants. (**A**–**D**) *TRN2* RNA expression pattern. (**A**) Wild type SAM and early leaf primordia. Note the expression in the SAM and at the tip of the young leaf to the left. The spot above the SAM corresponds to the tip of the next primordium which emerges from behind the SAM. (**B**) *TRN2* expression in the IM, an early floral bud and a stage 4 flower. (**C**) Close-up of a stage 3 flower. (**D**) Expression in stamen and carpels of a late flower (stage 7). *STM* transcription pattern in wild type (**E**) and *trn2-2*$_{3010}$ mutant vegetative SAMs (**F**); wild type (**G**) and *trn2-2*$_{3010}$ mutant (**H**) inflorescence meristems. (**I** + **J**) *CLV3* expression in the vegetative wild type (**I**) in comparison to the enlarged *trn2-2*$_{3010}$ mutant SAM (**J**). (**K** + **L**) *WUS* expression in the vegetative wild type (**K**) and the altered *trn2-2*$_{3010}$ mutant SAM (**L**). (**M**–**O**) *LFY* transcription in the 11 dag wild type (**M**) and similar stage *trn2-2*$_{3010}$ mutant SAM (**N**) in comparison to the florally induced wild type inflorescence and floral meristems (**O**). (**P**) Diagram with the results of 3 independent real-time PCR experiments to quantify the steady state levels of *STM*, *WUS* and *CLV3* transcripts in mutant trn2-2$_{3010}$ seedlings. Values are normalized to wildtype (=1) as indicated by the dotted line. Scale bars: A,E,G,I and N = 50 mm; B,C,D,F,H and O = 100 mm

expression of *CLV3* exhibits a preference for the L1/L2 layer but also extends to the uppermost cells of the L3 (Fletcher et al. 1999), *WUS* transcripts are confined to a few subtending *CLV3*-expressing cells in the L3 layer (Mayer et al. 1998). Although the *trn2-2*$_{3010}$ mutant meristem is enlarged relative to wild type, the *CLV3* and *WUS* expression domains show no major differences in size or position relative to wild type (compare Fig. 4I to J and K to L). This result is substantiated by quantitative real-time PCR experiments discussed below. Both markers therefore unequivocally argue against the central stem cell zone being increased in the *trn2-2*$_{3010}$ mutant relative to wild type.

To exclude that the change in SAM morphology in the *trn2-2*$_{3010}$ mutant is due to floral phase change transition, we performed RNA in situ hybridisation

experiments with the *LEAFY* (*LFY*) molecular marker. *LFY* is a meristem identity gene which is transcriptionally activated upon the floral transition. However, a comparison between *trn2-2$_{3010}$* seedlings and wild type controls depicted in Fig. 4M–O shows no significant difference in *LFY* transcriptional activity in the vegetative SAM between wild type (Fig. 4M) and mutant (Fig. 4N), whereas transcription is significantly increased after floral induction (Fig. 4O). This therefore rules out that floral induction accounts for the change in SAM shape observed in *trn2-2$_{3010}$* mutant seedlings.

Real time PCR experiments strongly support an increase in *STM* transcript levels in *trn2-2$_{3010}$* mutant seedlings. Student's *t*-test $P < 0.01$ values calculated from 3 independent experiments substantiate a 4-fold increase in *STM* transcript levels (4.0) in the mutant seedlings relative to wild type controls 11 days after germination (see diagram in Fig. 4P). Similar quantification did not substantiate a change in *WUS* transcripts (1.22). Although the amount of *CLV3* transcripts consistently appeared reduced by about 2-fold in *trn2-2$_{3010}$* mutant seedlings (0.54) compared with the level in wild type, *P* values close to 0.5 did not substantiate these differences as being significant. Taken together, the gene expression patterns and the quantitative real-time PCR data imply that the *STM* expression domain in the *trn2-2$_{3010}$* mutant SAM is increased relative to the central stem cell zone and that the enlargement of the shoot apex 11 days after germination consequently does not relate to an increased stem cell zone.

trn2 compensates for a loss of *STM* function

To analyse potential functional interactions between *TRN2* and *STM*, the *trn2-2$_{3010}$* allele was crossed into the *stm-1* and *stm-5* mutant backgrounds, strong and weak *stm* mutant alleles, respectively. In homozygous *stm-1* mutants, the SAM does not normally develop any leaves in contrast to the weak *stm-5* background where vegetative leaves are very occasionally produced (Endrizzi et al. 1996). For *stm-1 trn2-2$_{3010}$* double mutants, 30 from a total of 40 seedlings (75%) developed at least one leaf 8 days after germination and all double mutant progeny developed leaves by day 20 (see Table 2). In 19 *stm-1 trn2-2$_{3010}$* double mutant seedlings, leaves initiated from the base of the cotyledons (Fig. 5A), which were always fused due to lack of early *STM* activity (Long and Barton 1998). In the remaining 21 double mutant progeny single leaves or side shoots (Fig. 5B) arose laterally, from the outside of the fused base of the petioles instead of being initiated from the shoot apex and thus resembled *stm-1* mutant side shoots which are initiated after a long delay.

Table 2 Genetic interactions between *trn2* and *stm* mutants

Genotype	Total plant number	Fraction with leaves 8 DAG	Fraction with leaves 20 DAG
stm-1 (L*er*)[a]	49	0.0%	0%
stm-5 (L*er*)[a]	29	3.0%	55.0%
stm-1 (L*er*/Col)[b]	38	5.3%	39.5%
stm-5 (L*er*/Col)[b]	38	24.2%	71.9%
trn2-2$_{3010}$ stm-5 (L*er*/Col)[b]	40	75.0%	100%
trn2-2$_{3010}$ stm-1 (L*er*/Col)[b]	54	51.7%	100%

[a] L*er* background

[b] L*er*/Col hybrid background

A similar rescue of the *stm* mutant phenotype by *trn2-2$_{3010}$* was also observed in the weaker *stm-5* background where about 51% of *stm-5 trn2-2$_{3010}$* double mutant seedlings produced leaves by 8 days after germination, compared to only 3% in the *stm-5* single mutant. In contrast to combination with *stm-1*, leaves of *stm-5 trn2-2$_{3010}$* double mutants never initiated from outside the base of the cotyledon petioles but emerged internally to the cotyledons where the SAM normally resides in wild type (Fig. 5B). The weaker *stm-5* allele appears to be less responsive to the *trn2-2$_{3010}$* mutant background, a difference which may be due to the responding cell-types, which in *stm-1 trn2-2$_{3010}$* seedlings involves basal cells of the cotyledon petioles (Clark et al. 1996) but not remnant cells of the meristem domain.

As the *stm-1* or *stm-5* mutant alleles are in the L. *erecta* background, whereas the *trn2-2$_{3010}$* allele in Columbia, we had to exclude that rescue of the *trn2-2$_{3010}$* phenotype was due to the hybrid L*er*/Col background. Control crosses of *stm1* and *stm5* alleles and Col revealed that genetic background interactions couldn't solely account for the phenotype rescue, although *stm-1* and *stm-5* mutant seedlings initiated leaves more frequently in the L*er*/Col hybrid background than in the isogenic L*er* background. When normalized by the number of leaves in *stm1* and *stm5* hybrid L*er*/Col seedlings the presence of the *trn2-2$_{3010}$* allele still accounts for a 15-fold or 2-fold increase in leaf number in the *stm-1 trn2-2$_{3010}$* and *stm-5 trn2-2$_{3010}$*, respectively 8 days after germination (see Table 2). Therefore, the *trn2* background can partially compensate for a deficiency in *STM* function. Unfortunately, none of the double mutant progeny developed flowers,

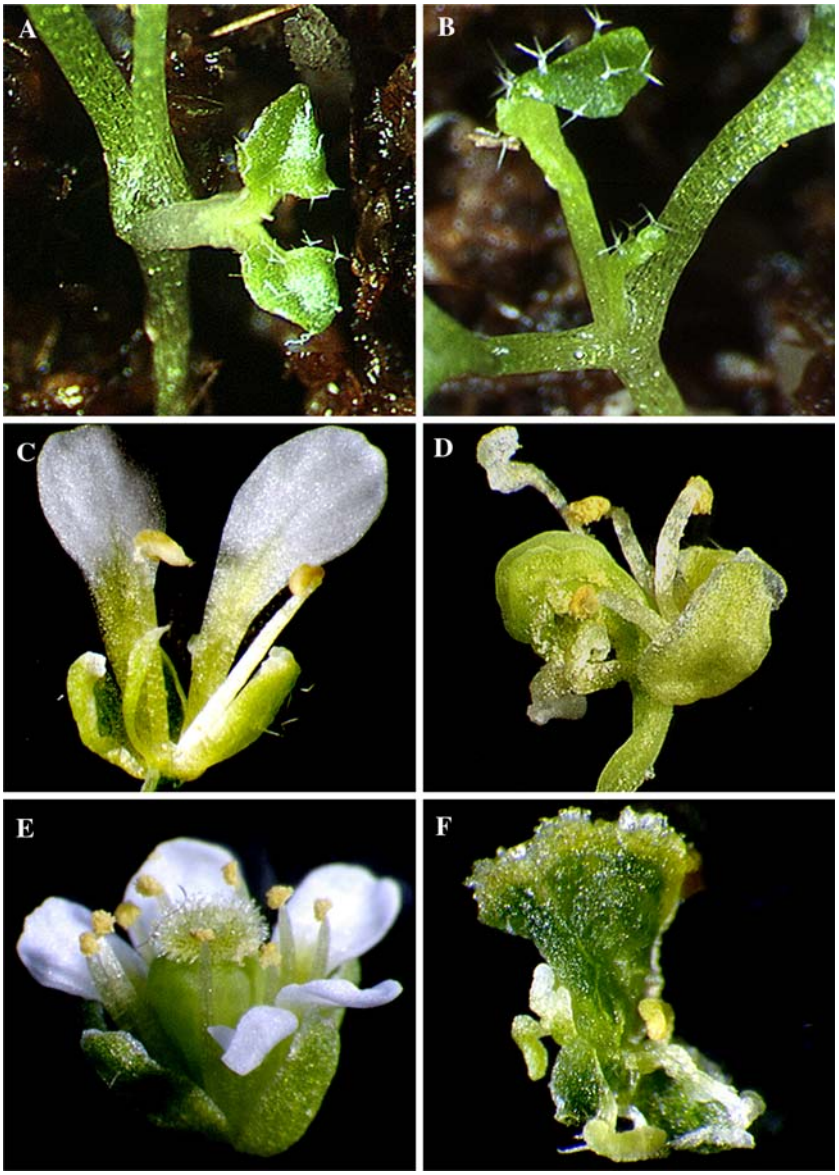

Fig. 5 Phenotype of double mutants between $trn2_{3010}$ and *stm*, *wus* and *clv3* mutants. (**A**) $trn2\text{-}2_{3010}$ *stm-1* double mutant at 10 dag. Note that leaves are borne from a secondary axis. (**B**) $trn2\text{-}2_{3010}$ *stm-5*. (**C**) *wus-1* flower with two stamens in comparison to a $trn2\text{-}2_{3010}$ *wus-1* double mutant flower (**D**) with several stamens surrounding a central twisted carpel. (**E**) *clv3-2* flower (**F**) double mutant $trn2_{3010}$ *clv3-2* flower comprised of multiple carpels and over-proliferating stigmatic tissue

which prevented a phenotypic analysis during the reproductive phase.

Genetic interactions with *WUS* and *CLV*

Although we observed no significant differences in *CLV3* and *WUS* expression patterns in the $trn2\text{-}2_{3010}$ mutant SAM compared with the wild type, we performed crosses between $trn2\text{-}2_{3010}$ and *wus-1* or *clv3-2* mutants. In contrast to $trn2\text{-}2_{3010}$ *stm* double mutants, we found no additional phenotype in $trn2\text{-}2_{3010}$ *wus-1* and $trn2\text{-}2_{3010}$ *clv3-2* mutants during the vegetative phase. However, some differences in flowers of double mutant plants were observed. Whereas carpels were completely absent in *wus-1* flowers (Fig. 5C) and only 1.6 stamens (compared to 6 in wild type) developed in the third floral whorl, all $trn2\text{-}2_{3010}$ *wus-1* flowers developed 2 carpels, which in contrast to $trn2\text{-}2_{3010}$ single mutants were seldom open (33%) and more usually fused (Fig. 5D). Consistent with the increased number of stamens (4.2 on average) in the third floral whorl, the *trn2* mutation may compensate for a premature consumption of stem cells in *wus-1* flowers. In contrast, the number of sepals and petals in the outer perianth whorls in $trn2\text{-}2_{3010}$ *wus-1* was closer in number to that of the *trn2* mutant rather than to *wus-1* single mutant flowers.

$trn2\text{-}2_{3010}$ *clv3-2* double mutant flowers also exhibited an additive phenotype not observed in single *clv3-2* or $trn2\text{-}2_{3010}$ plants: double mutant flowers had

reduced organ numbers in sepal, petal and stamen whorls, reminiscent of *trn2-2*$_{3010}$ single mutant flowers and in contrast to *clv3-2* single mutant flowers (Fig. 5E), there was no increase in the number of stamens. However, in the fourth whorl, where *trn2* loss-of-function interferes with the fusion of two carpels to the single style, double mutant flowers were comprised of multiple carpels, most of them fused (73%) as typically found in the *clv3-2* mutation. Supernumerary stem cells in *clv3-2* mutant floral meristems therefore not only led to the initiation of multiple carpels in the *trn2* background but also favoured their fusion to a single style which remained severely twisted. In addition to a style consisting of multiple carpels, over-proliferating callus-type tissue was observed at the tip of the style in all flowers (Fig. 5F). The quantification of floral organ number in the different single or double mutant backgrounds is shown in Table 1. Consistently, the novel phenotypes observed in *trn2-2*$_{3010}$ *wus-1* or *trn2-2*$_{3010}$ *clv3-2* double mutant flowers became evident towards the end of floral development and support the assumption that the *trn2* mutations may affect cellular decisions in the FM centre. In conclusion, all double mutants between *trn2-2*$_{3010}$ and *stm*, *wus* or *clv3* alleles implicate a role for *TRN2* in SAM function from early vegetative to late floral development.

Discussion

Starting from a genetic screen designed to identify changes in *STM* promoter activity, a new *trn2* mutant allele was isolated. It carries the same G to A nucleotide substitution as the previously identified *trn2-2* allele (Cnops et al. 2006), and was designated *trn2-2*$_{3010}$ to trace crosses performed with the new isolate here. The mutation results in a G to E amino acid exchange in the characteristic second large extra cellular loop of tetraspanin proteins. The re-isolation of a *trn2* mutant in a screen designed to identify changes in the *STM-GUS* expression pattern led to a careful inspection of the SAM histology in the *trn2-2*$_{3010}$ mutant, which is recovered in *trn2-2*$_{3010}$/*trn2-1* or *trn2-2*$_{3010}$/*trn2-2* trans-heterozygotes. In addition to the use of molecular markers, double mutants between *trn2-2*$_{3010}$ and *stm-1, stm-5*, *clv3-2* or *wus-1* were created.

A peculiarity of *trn2-2*$_{3010}$ seedlings was an altered shape and an enlargement of the shoot apex, which contains about 40% more cells than wild type. The use of *LFY*, a molecular marker of floral induction, ruled out that the change in SAM morphology is caused by early floral induction. In the absence of functional TRN2 protein, the SAM therefore acquires an atypical morphology during early seedling development. Activity of the *STM:GUS* transgene marker and the transcription pattern of the endogenous *STM* gene indicate that cells within the larger *trn2* mutant apex maintain meristematic identity. This enlargement of the SAM is reflected in a 4-fold increase in the amount of *STM* transcripts detected in *trn2-2*$_{3010}$ seedlings relative to wild type Columbia controls in quantitative PCR experiments but we cannot exclude that part of this increase is due to higher *STM* mRNA steady state levels. A slight discrepancy exists between the enlarged GUS activity domain in whole mount seedlings and the more restricted expression of *STM* in RNA in situ hybridisations, although in briefly stained ultra-thin sections, the *STM-GUS* marker is also SAM-specific. One explanation may exist on the level of stability of the endogenous *STM* RNA relative to the GUS transcript. To the best of our knowledge there are no experimental data in support of *KNOX* genes such as *STM* being directly targeted by micro RNAs. However, evidence exists that *BREVIPEDICELLUS* (*BP*), the closest relative of *STM* in the *Arabidopsis* genome is repressed by RNA polymerase RDR6, synergistically with *ASYMMETRIC LEAVES1* and *2* during leaf development (Li et al. 2005). Therefore, it is conceivable that *STM* RNA transcripts are prone to post-transcriptional control outside the SAM, whereas chimeric GUS transcripts are not. The *STM-GUS* marker gene contains part of the 5' untranslated sequences of the *STM* gene. These *STM* 5′UTR sequences in front of the GUS coding region could also explain differences in expression between whole mounts and ultra-thin sections, if post-transcriptional control is not absolutely specific and allows translations of low levels of GUS enzyme.

Strikingly, the increase in the *STM* expression domain is not reflected in altered expression patterns of the *WUS* and *CLV3* molecular markers (Mayer et al. 1998; Fletcher et al. 1999), which both delineate cellular identities in the central stem cell zone. Based on RNA in situ hybridisations, neither the *WUS* domain, nor the overlying *CLV3* domain was significantly altered in *trn2* meristems relative to wild type. Although real-time RT PCR experiments substantiated a slight, 2-fold reduction in the amount of *CLV3* transcripts, this was not reflected in either the size of the expression domain or a by significant effect on *WUS* transcription. Stem cell homeostasis in the *Arabidopsis* SAM is controlled by a feedback loop between WUS promoting stem cell fate, and CLV signalling, which restricts the number of stem cells by antagonizing *WUS* activity (reviewed in Waites and Simon 2000; Schoof

et al. 2000). Based on the *WUS* or *CLV3* markers, only minor changes in the central stem cell zone result from absence of the *TRN2* function. Consequently, an increased stem cell population as in *clv* mutants cannot account for the SAM enlargement.

In consequence, the *TRN2* deficiency primarily affects the peripheral zone of the SAM, a conclusion consistent with the *trn2* phenotype of severe dwarfism with twisted and malformed lateral organs (Cnops et al. 2006). In contrast, *trn2* cotyledons which are no derivatives of the SAM (Laux and Jürgens 1997) remain unaffected in size and shape. The *trn2* phenotype thus reflects a malfunction of the shoot meristem. Careful analysis of the *trn2* phenotype in leaves showed that both cell proliferation as well as cell differentiation are affected, which relates to aberrant venation patterns and asymmetric leaf growth (Cnops et al. 2006). Earlier studies indicated that the radial patterning of the root meristem was incomplete in *trn2* mutant plants (Cnops et al. 2000) and cell fates were inappropriately specified with most irregularities seen in determined/differentiated cells such as the epidermal/lateral root cap cell files. These data provide clear evidence that *TRN2* contributes to cell fate decisions in the root meristem. The new finding, here, that the peripheral zone in the shoot apex is enlarged in *trn2* mutant plants suggests a similar contribution in the SAM.

Down-regulation of *STM* is the earliest signifier for the acquisition of primordial fate (P_0) (Long et al. 1996). In the absence of additional markers, we cannot discriminate whether cells at the periphery of the *trn2* SAM are released for terminal differentiation in an appropriate timely or spatial fashion, or whether cells within the peripheral zone of the SAM overproliferate. No obvious change in phyllotaxy was detected; positional information for the specification of founder cells for new lateral organs therefore is still correctly provided and perceived in the *trn2* meristem. In contrast, the enlargement of the *trn2* SAM is reflected in severe distortions in symmetry, shape or size of lateral organs. However, the absence of leaf portions, up to one half of the total leaf lamina (Cnops et al. 2006) suggests that early steps in leaf anlagen development are also affected. These deficiencies are reminiscent of clonal sectors obtained during analyses to estimate the number of primordial founder cells at the periphery of the *Arabidopsis* SAM (Irish and Sussex 1992). This aspect of the *trn2* phenotype therefore substantiates the fact that the *Arabidopsis* tetraspanin-like protein TRN2 contributes to cellular decisions at the SAM periphery. This is not only consistent with the acquisition of abnormal cell fates in the root meristem but also with changes in the SAM. This assumption is also compatible with double mutant analyses showing *trn2* to be epistatic to *asymmetric leaf1* (*as1*) (Cnops et al. 2006). *AS1* is activated in the P_1 leaf significantly later than the down-regulation of *STM* in P_0 (Byrne et al. 2002). Whereas Cnops et al. (2006) identified a synergism between *TRN2* and *AS1* during leaf development including an altered venation pattern in *as1/trn2* double mutants, we have shown here that *trn2* loss-of-function has additional consequences within the SAM. Consistently, both data sets implicate *TRN2* in contributing to cellular decisions during shoot development, but the data here imply that the primary function of *TRN2* may reside in the SAM.

Genetic interactions

Double mutant analyses substantiated the histological changes observed in the *trn-2-2*$_{3010}$ shoot apex on the functional level. During early seedling development, the *trn2-2*$_{3010}$ mutation rescued the strong *stm-1* allele and suppressed the weaker *stm-5* allele. In both double mutant backgrounds, leaves or new side shoots were initiated more rapidly than in either *stm* single mutant (Endrizzi et al. 1996). The rescue was more pronounced with the strong *stm-1* allele than with the weaker *stm-5* background, which slowly initiates leaves on its own. The compensation observed if the strong *stm-1* allele is combined with the *trn2* mutant argues that the rescue does not relate to residual *STM* function but implicates *trn-2* in another pathway. Morphological changes in the shoot apex may not result from an altered *STM* transcription domain but the altered *STM* promoter activity presumably misinterprets information provided by another pathway involving *TRN2*. Encoding a membrane-associated tetraspanin protein, *TRN2* cannot directly account for altered *STM* promoter activity without involving downstream signalling. Concerning the signalling pathway, it will be interesting to elucidate the contribution of *TRN1* which encodes a Leucine-rich repeat (LRR) protein of the ribonuclease inhibitor subfamily and acts in the same pathway as *TRN2* (Cnops et al. 2006). Both the enlarged vegetative shoot apex and the partial rescue of the *stm* mutant phenotype in the *trn2* background suggest that *TRN2* may be involved in restricting meristem identity. This assumption would also be compatible with the lack of leaf segments (Cnops et al. 2006, see Fig. 2C), when cells normally recruited as leaf founder cells according to their position are not released for primordial fate in a timely fashion.

In contrast to double mutants with *stm* alleles, no novel phenotypes during vegetative development were observed in combinations of *trn2-2*$_{3010}$ with the *wus-1* or the *clv3-2* alleles. The phenotype of *trn2-2*$_{3010}$ *wus-*$_{1}$ double mutants was additive, similar to that of *wus-1* seedlings with twisted leaves. During the reproductive phase, however, the double mutant *trn2-2*$_{3010}$ phenotype was epistatic to that of *wus-1* and flowers developed more stamens in the third whorl and generally carpels in the fourth whorl, which are lacking in *wus-1* single mutants (Laux et al. 1996). If the *trn2-2*$_{3010}$ *wus-1* double mutant FM is enlarged similar to the vegetative SAM in *trn2* seedlings, it might contain a greater number of meristematic cells, which is not completely consumed through the differentiation of anlagen of outer whorl organs as in the *wus-1* single mutant (Laux et al. 1996). Such cells could remain competent for the development of reproductive organs in the inner whorls and explain the increase in stamen number and carpel development. In support of this assumption, the combination of *trn2-2*$_{3010}$ with the *clv3-2* mutation showed no novel phenotype during vegetative or early reproductive development. During early floral stages, the *trn2-2*$_{3010}$ phenotype was again epistatic to that of *clv3-2* and organ numbers in the three outer whorls of sepals, petals and stamens resembled those in *trn2-2*$_{3010}$ mutant flowers and not the increased numbers in *clv3-2* mutant flowers. However, this changed at the end of flower development; instead of 2 unfused carpels in *trn2-2*$_{3010}$ single mutants, all *trn2-2*$_{3010}$ *clv3-2* double mutant flowers contained on average more than 5 carpels, which were generally fused to a single, twisted style. In consequence, double mutant *trn2-2*$_{3010}$ *wus-1* or *trn2*$_{3010}$ *clv3-2* flowers showed *trn2*-specific reductions in organ number in the outer whorls of sepals and petals, even decreasing stamen number relative to *clv3-2* alone, whereas additional organs were formed in the inner carpel whorl in both double mutant combinations.

Carpel number most sensitively reflects changes in stem cell homeostasis and the number of stem cells is thought to be increased in *clv* mutants (Clark et al. 1997; Fletcher et al. 1999) and reduced in *wus* mutants (Laux et al. 1996). It is striking therefore, that the *trn2* mutations causes a reduction in organ number in the outer floral whorls of *clv3-2* and *wus-1* flowers but allows the development of additional organs in the inner carpel whorl. One explanation may be that sepal, petal or stamen founder cells are recruited from the peripheral zone of the FM, whereas determinacy of the flower involves the loss of stem cell fate in the centre of the FM at the end of floral development. This is achieved through down-regulation of *WUS* by the organ identity C-function gene *AGAMOUS* (Lenhard et al. 2001; Lohmann et al. 2001). Starting from a limited pool of meristematic cells in the FM, which is not renewable in *wus-1* single mutants, any reduction in cell numbers released for differentiation into floral organs in *trn2-2*$_{3010}$ *wus-1* double mutants could save pluripotent cells for the recruitment into stamens or carpels in the FM centre. Conversely, the supernumerary stem cells in *clv3-2* mutant FMs have few consequences in the peripheral zone where founder cells for sepals, petals or stamens are recruited. The reduced numbers of sepals, petals or stamens in *trn2-2*$_{3010}$ *clv3-2* double mutants, therefore, may reflect the *TRN2* deficiency in the peripheral zone and consequently be different to carpel development, which involves the termination of stem cell fate. The *clv3-2* mutation causes a surfeit of pluripotent cells in the FM; according to positional or developmental cues, these cells are destined to inititate carpels in the late FM. As the *trn2* mutant background allows differentiation, an excessive stem cell number may result in a multiplicity of carpels or callus-type tissue as observed in flowers of double mutants with *clv3-2*. In conclusion, all the data implicate a role for a membrane-bound plant tetraspanin protein in contributing to cellular decisions in the SAM.

Acknowledgements We thank Melanie Cole, Pia Neyt and Wilson Ardiles-Diaz for excellent technical assistance. This research was funded by the Deutsche Forschungsgemeinschaft through SFB 572. W-H. Chiu was a member of the Graduate College ''Molecular Analysis of Plant Development'' at the University of Cologne.

References

Bradley D, Carpenter R, Sommer H, Hartley N, Coen E (1993) Complementary floral homeotic phenotypes result from opposite orientations of a transposon at the plena locus of *Antirrhinum*. Cell 72:85–95

Byrne ME, Simorowski J, Martienssen RA (2002) *ASYMMETRIC LEAVES1* reveals knox gene redundancy in *Arabidopsis*. Development 129:1957–1965

Carland FM, McHale NA 1996. *LOP1*: a gene involved in auxin transport and vascular patterning in *Arabidopsis*. Development 122:1811–1819

Chomczynski P, Sacchi N (1987) Single-step method of RNA isolation by acid guanidinium thiocyanate-phenol-chloroform extraction. Analytical Biochemistry 162:156–159

Clark SE, Jacobsen SE, Levin JZ, Meyerowitz EM 1996. The *CLAVATA* and *SHOOT MERISTEMLESS* loci competitively regulate meristem activity in *Arabidopsis*. Development 122:1567–1575

Clark SE, Williams RW, Meyerowitz EM (1997) The *CLAVATA1* gene encodes a putative receptor kinase that controls shoot and floral meristem size in *Arabidopsis*. Cell 89:575–585

Cnops G, Wang X, Linstead P, Van Montagu M, Van Lijsebettens M, Dolan L (2000) *Tornado1* and *tornado2* are required for the specification of radial and circumferential pattern in the *Arabidopsis* root. Development 127:3385–3394

Cnops G, Neyt P, Raes J, Petrarulo M, Nelissen H, Malenica N, Luschnig C, Tietz O, Ditengou F, Palme K, Azmi A, Prinsen E, Van Lijsebettens M (2006) The *TORNADO1* and *TORNADO2* genes have a function in several patterning processes during early leaf development in *Arabidopsis thaliana*. Plant Cell 18:852–866

Endrizzi K, Moussian B, Haecker A, Levin JZ, Laux T (1996) The *SHOOT MERISTEMLESS* gene is required for maintenance of undifferentiated cells in *Arabidopsis* shoot and floral meristems and acts at a different regulatory level than the meristem genes *WUSCHEL* and *ZWILLE*. Plant J 10:967–979

Ewing B, Hillier L, Wendl MC, Green P (1998) Base-calling of automated sequencer traces using phred. I. Accuracy assessment. Genome Res 8:175–185

Fletcher JC, Brand U, Running MP, Simon R, Meyerowitz EM (1999) Signaling of cell fate decisions by *CLAVATA3* in *Arabidopsis* shoot meristems. Science 283:1911–1914

Hemler ME (2005) Tetraspanin functions and associated microdomains. Nat Rev Mol Cell Biol 6:801–811

Irish VF, Sussex IM (1992) A fate map of the *Arabidosis* embryonic shoot apical meristem. Development 115:745–753

Jackson D (1991) In situ hybridization in plants. In: Bowles DJ, Gurr SJ, McPerson M (eds), Molecular plant pathology: A practical approach. Oxford University Press, Oxford, pp 163–174

Kasajima I, Ide Y, Ohkama-Ohtsu N, Hayashi H, Yoneyama T, Fujiwara T (2004) A protocol for rapid DNA extraction from *Arabidopsis thaliana* for PCR analysis. Plant Mol Biol Rep 22:49–52

Kirch T, Simon R, Grunewald M, Werr W (2003) *The DORNRÖSCHEN-ENHANCER OF SHOOT REGENERATION1* gene of *Arabidopsis* acts in the control of meristem ccll fate and lateral organ development. Plant Cell 15:694–705

Konieczny A, Ausubel FM (1993) A procedure for mapping *Arabidopsis* mutations using co-dominant ecotype-specific PCR-based markers. Plant J 4:403–410

Laux T, Mayer KF, Berger J, Jürgens G (1996) The *WUSCHEL* gene is required for shoot and floral meristem integrity in *Arabidopsis*. Development 122:87–96

Laux T, Jürgens G (1997) Embryogenesis: a new start in life. Plant Cell 9:989–1000

Lenhard M, Bohnert A, Jürgens G, Laux T (2001) Termination of stem cell maintenance in *Arabidopsis* floral meristems by interactions between *WUSCHEL* and *AGAMOUS*. Cell 105:805–814

Levy S, Shoham T (2005) The tetraspanin web modulates immune-signalling complexes. Nat Rev Immunol 5:136–148

Li H, Xu L, Wang H, Yuan Z, Cao X, Yang Z, Zhang D, Xu Y, Huang H (2005) The Putative RNA-dependent RNA polymerase RDR6 acts synergistically with ASYMMETRIC LEAVES1 and 2 to repress BREVIPEDICELLUS and MicroRNA165/166 in *Arabidopsis* leaf development. Plant Cell 17:2157–2171

Livak KJ, Schmittgen TD (2001) Analysis of relative gene expression data using real-time quantitative PCR and the 2(-Delta Delta C(T)) Method. Methods 25:402–408

Lohmann JU, Hong RL, Hobe M, Busch MA, Parcy F, Simon R, Weigel D (2001) A molecular link between stem cell regulation and floral patterning in *Arabidopsis*. Cell 105:793–803

Long JA, Moan EI, Medford JI, Barton MK (1996) A member of the *KNOTTED* class of homeodomain proteins encoded by the STM gene of *Arabidopsis*. Nature 379:66–69

Long JA, Barton MK (1998) The development of apical embryonic pattern in *Arabidopsis*. Development 125:3027–3035

Mayer KF, Schoof H, Haecker A, Lenhard M, Jürgens G, Laux T (1998) Role of *WUSCHEL* in regulating stem cell fate in the *Arabidopsis* shoot meristem. Cell 95:805–815

Olmos E, Reiss B, Dekker K (2003) The *ekeko* mutant demonstrates a role for tetraspanin-like protein in plant development. Biochem Biophys Res Commun 310:1054–1061

Reinhardt D, Pesce ER, Stieger P, Mandel T, Baltensperger K, Bennett M, Traas J, Friml J Kuhlemeier C (2003) Regulation of phyllotaxy by polar auxin transport. Nature 426:255–260

Sanger F, Nicklen S, Coulson AR (1977) DNA sequencing with chain-terminating inhibitors. Proc Natl Acad Sci USA 74:5463–5467

Schoof H, Lenhard M, Haecker A, Mayer KF, Jürgens G, Laux T (2000) The stem cell population of *Arabidopsis* shoot meristems in maintained by a regulatory loop between the CLAVATA and WUSCHEL genes. Cell 100:635–644

Sussex IM (1989) Developmental programming of the shoot meristem. Cell 56:225–229

Waites R, Simon R (2000) Signaling cell fate in plant meristems. Three clubs on one tousle. Cell 103:835–838